Australian Journal of Basic and Applied Sciences, 4(11): 5599-5613, 2010
ISSN 1991-8178

Length Effects on Capacitance Measurements of a Cylindrical Cell Probe

[1]M. Sharifian and [2]H. Golnabi

[1]Physics Department, Tehran North Branch, Islamic Azad University
[2]Institute of Water and Energy, Sharif University of Technology
P. O. Box 11155-8639, Tehran, Iran

Abstract: Using two different capacitive cell probes; and monitoring capacitance and resistance values of the air and water liquids, the cell length and conductance effects of the water liquids are studied. Variations of the dielectric air capacitance and reactance capacitance parameter of liquids with cylinder length are investigated. In another study the probe length affects on the capacitance and resistance measurements for the liquid filling process are investigated. Different theories are also developed to calculate the capacitance values for the constructed probes. Capacitance per unit length from the Coulomb theory is different from the Gauss law that is a constant value. Measured air capacitance of 24.7 pF (15.3 pF) and calculated ones Gauss, 19.39 pF (9.66 pF), and Coulomb 24.7 pF (15.3 pF) for the long (short) probe are obtained. A comparison of the experimental air capacitance results with the Coulomb theory shows a relative error percentage of 10.58% for the long probe and an error of 27.32% for the short probe. For liquid samples, there is a good agreement between the measured conductivity results by the EC and the two cylindrical cell probes using LRC module. In particular for the distilled, mineral, tap and boiled water samples the relative errors for the short and long cylindrical probes are lower than 2%, which is a good agreement for such measurements. Obtained results verifies that the reported cylindrical sensor could be effectively implemented for the study of low conducting liquids such as regular water and dilute water solutions.

Key word: Cylindrical cell, Capacitance, Conductance, Resistance, Length, Water

INTRODUCTION

Determination of physical parameters of liquids such as electrical conductivity and capacitance, in particular for water samples, can be a great tool in characterization and analysis of such substances. Although ultra pure water is a very good dielectric medium, but natural impurities found in regular water can transform it to a conductor. Salts and other contaminates in water can dissociate into components called ions, which are mostly responsible for the electrical conduction. In recent years capacitive probes have found many applications in different fields and extensive works have been done to develop different probe arrangements and readout circuits for high-quality operation (Fasching *et al.,* 1994; Guo *et al.,* 2000; Huang *et al.,* 1988; Huang *et al.,* 1988; Light *et al.,* 2005; Rodjegard and Loof, 2005).

Since capacitance is basically a small value as a result a minor change in such parameter can be converted into a reasonable output voltage or frequency changes in readout circuits. In operation plane electrodes, cylindrical and differential geometries are developed and used in a variety of applications (Tsamis and Avaritsiotis, 2005; Kasten *et al.,* 2000; McIntosh *et al.,* 2006; Moe *et al.,* 2000; Ahn *et al.,* 2005). Depending on the electrode configuration invasive (direct contact between the metal electrode and liquid) and non-invasive (no contact between the metal electrode and liquid) arrangements are developed depending on the application requirements.

It is shown that non-invasive type electrode arrangement are more suitable for dielectric capacitance measurements while the invasive electrode structure is more effective for the investigation of the conductance property of the inter-electrodes gap samples. Such invasive cylindrical cell probes can be effectively used for the monitoring dielectric capacitance of air sample and reactance capacitance values of the water liquids as well. In this respect design and performance of a cylindrical capacitive sensor to monitor the electrical properties of liquids was introduced in the previous report (Golnabi and Azimi 2008) In the following study simultaneous measurements of the resistance and capacitance by using a cylindrical sensor system was reported

Corresponding Author: M. Sharifian, Physics Department, Tehran North Branch, Islamic Azad University

(Golnabi and Azimi, 2008). In another report (Behzadi and Golnabi, 2009) monitoring temperature variation of reactance capacitance of water using such a cylindrical cell probe is described. In reported experiments a three-electrode design with a guard rings is used for the experimental measurements, which revealed new scientific results. However in those reports and even in related literature the role of cell probe length in the dielectric capacitance and reactance capacitance variations are not fully depicted.

Even though three-electrode design used in the previous reports works well for the case of small capacitance measurements canceling the stray capacitance effects, however the design of the electrodes is more complicated and as a result a simpler two-electrode design is developed for the purpose of the research conducted here. In this study the new design, which is simpler and more reproducible in electrode configuration is used to construct two similar capacitive cell probes with same materials for the electrodes with only length difference. In addition, a new measuring system with a higher capability is used for the simultaneous capacitance and resistance measurements. One important parameter involved in such investigations is the cell length effect, which is investigated here by the new proposed cylindrical cell probes. Our goal is to study the dielectric and reactance capacitance parameter of liquids with cylinder length as a variable for the air gap and when gap is partly-filled or full-filled with different water samples. Besides experimenting such effects another goal is to develop a more precise theory in order to calculate the air capacitance values for the constructed probes and compare theoretical results with the measured experimental values.

2. Theory of Capacitance Calculation:

In our theoretical developments we consider the simple Gauss Law and the more general formula of the Coulomb theory:

2.1. Gauss's law:

Using Gauss's law the capacity of a long cylindrical capacitor can be obtained from

$$C = \frac{2\pi\varepsilon L}{Ln\frac{b}{a}} \tag{1}$$

where ε is the permittivity of the gap dielectric medium. Here a is the inner electrode radius, b outer electrode radius, and L is the capacitor length as shown in Fig.1. However Eq. (1) is only valid when L>> a,b and a more accurate formula should be used for the case of small L. Several problems such as edge effect, can cause deviation in the actual capacity from the given formula in Eq. (1). For this reason, various attempts have been made to reduce errors due to the limited size effects. One simple remedy has been the use of a Kelvin guard-ring (Golnabi, 2000) in which the main inner electrode is shielded by a grounded guard-ring electrode.

2.2. Coulomb's law:

In Coulomb method, we use an electrical potential difference, and according to:

$$C = \frac{Q}{\varphi_{ab}} \tag{2}$$

the capacitance value C for a given charge value of Q on each electrode can be obtained. In the cylindrical coordinates, electrical potential at each point in space between the two capacitor electrodes can be derived from Eq.(3) and with the integration over the cylinder capacitor length one can write

$$\varphi_r^{(i)} = -\frac{Q}{4\pi\varepsilon(2\pi\rho' L)}\left(\int \rho' Ln(z - z' + \sqrt{\rho'^2 + (z-z')^2 + 2\rho\rho'\cos(\varphi') + \rho^2}) \right]_{-\frac{L}{2}}^{+\frac{L}{2}} d\varphi' \Bigg), \tag{3}$$

where L is the length of the cylinder probe. Eq.(3) can be written as

$$\varphi_r^{(i)} = -\frac{Q}{8\pi^2\varepsilon L}\left(\int Ln\left(\frac{z - \frac{L}{2} + \sqrt{\rho'^2 + (z-\frac{L}{2})^2 + 2\rho\rho'\cos(\varphi') + \rho^2}}{z + \frac{L}{2} + \sqrt{\rho'^2 + (z+\frac{L}{2})^2 + 2\rho\rho'\cos(\varphi') + \rho^2}}\right) d\varphi' \right), \tag{4}$$

Thus the electrical potential at radius, ρ , can be obtained from

$$\varphi_r(z,\rho,L) = -\frac{Q}{8\pi^2\varepsilon L}\Bigg(\int Ln\left(\frac{z-\frac{L}{2}+\sqrt{a^2+(z-\frac{L}{2})^2-2\rho a\cos(\varphi')+\rho^2}}{z+\frac{L}{2}+\sqrt{a^2+(z+\frac{L}{2})^2-2\rho a\cos(\varphi')+\rho^2}}\right)d\varphi' + \int Ln\left(\frac{z-\frac{L}{2}+\sqrt{b^2+(z-\frac{L}{2})^2-2\rho b\cos(\varphi')+\rho^2}}{z+\frac{L}{2}+\sqrt{b^2+(z+\frac{L}{2})^2-2\rho b\cos(\varphi')+\rho^2}}\right)d\varphi' \Bigg) \tag{5}$$

Where the potential difference is determined from the relation

$$\varphi_{ab} = \varphi_r(z,a,L) - \varphi_r(z,b,L), \tag{6}$$

For the finite length the electrical potential difference between two cylinders with radius of a,b (assume b>a). Finally we can calculate the electrical capacitance from Eq. (9) such as

$$C = 8\pi^2\varepsilon L\left[\int Ln\left(\frac{z-\frac{L}{2}+\sqrt{a^2+(z-\frac{L}{2})^2-2a^2\cos(\varphi')+a^2}}{z+\frac{L}{2}+\sqrt{a^2+(z+\frac{L}{2})^2-2a^2\cos(\varphi')+a^2}}\right)d\varphi' - \int Ln\left(\frac{z-\frac{L}{2}+\sqrt{b^2+(z-\frac{L}{2})^2-2b^2\cos(\varphi')+b^2}}{z+\frac{L}{2}+\sqrt{b^2+(z+\frac{L}{2})^2-2b^2\cos(\varphi')+b^2}}\right)d\varphi'\right]^{-1} \tag{7}$$

3. Conductance Consideration:

Physical and chemical properties of water results from strong attraction that hydrogen atoms have for each other in water molecules. In most cases, ions in water are considered as impurities especially when referring to pure water, while in other aqueous solutions such as hydrochloric acid or sodium hydroxide, the ions define the actual chemical deposition. Water molecules are generally in continuous motion, even at low temperatures and when two water molecules collide, a hydrogen ion is transferred from one molecule to the other. The other molecule that losses the hydrogen ion becomes negatively charged hydroxide ion. The molecule that gains the hydrogen ion becomes a positively charged hydrogen ion and this process is commonly called the self-ionization of water. In fact at room temperature (25 ˚C), each concentration of hydrogen ions and hydroxide ions is only of the order of 1×10^{-7}M, and as a result this dissociation allows a minute electrical current to flow. The current flow is in the range of 0.05 μS/cm at room temperature. It is important to note that the amount of $(H)^+$ and $(OH)^-$ ions are approximately equal and this solution is described as a neutral solution. In other aqueous solutions, the relative concentrations of these ions are unequal and one ion is increased by one order of magnitude while the other one shows some decrease, but the relationship is constant and the ion product is always constant given by K_w, which is called the ion-product constant for water.

For the case of liquid filling the conductance effect of the liquid gap medium must be taken into consideration. Depending on the capacitance electrode configuration of the sensor the equivalent circuit can be considered for the case of invasive (direct contact between the metal electrode and liquid), and non-invasive (no contact between the metal electrode and liquid) sensors. In a simple form if we consider a uniform liquid with the given permittivity and conductivity, the equivalent circuits for the case of non-invasive and invasive sensors must be considered in analysis. It must be mentioned that the given capacitance value is the measured value by the charge transfer or resonance reading circuit and fluid capacitance must be deduced from the measured capacitance values for both readout modules.

Also noted that the capacitance sensing is affected by the conductivity variations of the components. This conductivity problem has been the main concern in the field of dielectric measurements and several attempts

have been made to compensate for such variation and for a simple case the effect of conductivity is presented by a resistive element in parallel with the probe capacitance. However, for sensors using non-invasive electrodes and those measuring two-component fluids; sensor systems must be represented by more complex equivalent circuit models. As a result an investigation into the effects of component conductivity should be done for precise measurements.

In general a variety of techniques have been employed for measuring the absolute and relative capacitance changes. Oscillation, Resonance, charge/discharge, AC bridge, and capacitive-to-phase conversion are the most common methods for such capacitance measurements. Since the PC-5000 (SANWA) module employed here uses the charge/discharge (C/DC) circuit, therefore, this method is described briefly here. The charge/discharge operation is based on the charging of an unknown capacitance under study C_x to a voltage V_c via a CMOS switch with resistance R_{on} and then discharging this capacitor into a charge detector via a second switch and C_x can be determined. In resonance method the capacitance value can be obtained from the relation. The LCR module uses the resonance method in which the capacitance value can be obtained from the relation

$$C = \frac{1}{\omega^2 L} = \frac{1}{4\pi^2 f^2 L} \tag{8}$$

where L is the series inductance and f is the frequency of the measuring module. The LCR module operates based on the balanced bridge circuit in which the impedence can be determined for the resistance and reactance values.

The capacitance measurements for the cylindrical probe depend on the permittivity, ε, of the liquid and its resistance factor that depends only on the conductivity, σ, of the liquid. Thus we can write

$$C_x = g_1\ [\varepsilon(t,f,T)], \tag{9}$$

$$R_x = g_2\ [\sigma(t,f,T)]. \tag{10}$$

The dielectric capacitive part of C is obtained only by the insulation of the electrodes and reducing the conductivity effect. It must be pointed out that both the permittivity ε and conductivity, σ also vary with temperature, time, and measuring frequency. In general the measured capacitance is a function of different parameters as given by

$$C_m = g\ [\varepsilon(t,f,T),\ \sigma(t,f,T),\ G] \tag{11}$$

where, C_m also varies with time t, frequency f, temperature T, and the probe geometry factor of G. In practice it is hard to perform a single measurement to evaluate the variation of all of these parameters on the measured capacitance. As a result, there are some ambiguities in the L effect and as a result G variation, which led us to follow up on this topic.

For the case of non-invasive sensors, in measuring capacitance of a liquid, the effect of resistive component is usually very small because of the dielectric insulator. For the invasive sensors, however, the effect of R_x on the measurement of C_x can not be neglected and the effect of conductivity of the liquid must be considered in analysis. Hence, in Charge/discharge method the effect of R_x can be negligible if the turn on resistance of the charge switch, R_{on}, is small compared with R_x, and if the discharge time, which is determined by the switching-on time of the resistance of the discharging switch, is short compared with the time constant given by R_xC_x. As mentioned when R_x is not negligible in analysis then it must be considered as reactance term in capacitance measurements.

4. Experimental Arrangement:

In this experiment a cylindrical geometry is chosen for the probe and aluminum material is used as the capacitor tube electrodes as shown in Fig.1. The diameter of the inner solid electrode is about 18 mm and the inner diameter of the outer electrode is about 24 mm and has a thickness wall diameter of about 6 mm. Both electrodes are machined from the same type aluminum rod. Two measurement leads are connected to the inner electrode and outer electrode, respectively. Two cell probes as shown in Fig.1 are constructed with the similar structure with the effective length of 5 and 10 cm, which are referred to as short and long probes, respectively. The overall height of the probe is about 14 cm (long probe) while the active probe has an effective length of about 7cm (short probe). The radial gap between the two tube electrodes for filling medium is about 3 mm, and the overall diameter of the probe is about 44 mm. The cylindrical gap volume measured when filled with water for the short sensor (5cm-length) is 10 cc and for the long one (10 cm-length) is 20 cc.

Experimental system in general includes a sensing probe and a measuring module. Our experimental setup is a simple one, which uses the capacitive sensing probe and alternatively a different measuring module as shown in Fig.2. It includes the cylindrical capacitive sensor, either a digital multimeter (DMM) module (SANWA, PC 5000), that can be interfaced to a PC or a LCR (Yuke-816, Good Will Instrument, Gw Instek) measuring module. The first measuring module DMM (SANWA) provides a function for capacitance measurements using the charge/discharge method and capacitance in the range of 0.01 nF to 9.99 mF can be measured with a resolution of about 0.01 nF. The nominal input impedance of the DMM is about 10 MΩ and 30 pF. The specified accuracy of the SANWA module for 50.00-500.0 nF capacitance range is about ± (0.8 % rdg+3dgt) and ± (2 % rdg+3dgt) for the 50.00 μF range. The software (PC Link plus) allows one to log measuring data into PC through RS232 port with digital multimeter PC series. More details about the SANWA module can be found in the technical instructions (Sanwa at web site: [http://www.sanwa-meter.co.jp/overseas/]).

The second instrument includes LCR-816, 2kHz high precision LCR meter and a LCR-06A measuring probe. It uses the structure of four wires measurement, which allows accurate and stable measurements and avoids mutual inductance and interference from measurement signals, noise and other factors inherent with other types of connections. It is easy to operate the device by using the main menu, which consists of four top level menus, OFFSET, SORT, SETTING, and CALIBRATION options. Four combinations of two parameters can be measured and displayed that could be parameters L (Inductance) and Q (quality factor), C (capacitance) and D (dissipation factor), C and R (resistance) or R and Q. Beside selected pair the meter also shows the measurement frequency.

Usually determination of C and R pair is the goal in our experimental measurements. In this configuration LCR meter displays the C, R at measured frequency and measurements can be performed in either series or parallel equivalent circuit. Capacitors less than 10 pF are measured in parallel mode at operating frequency of 100 kHz. Capacitors from 10 pF to 400 pF can be measured in series or parallel at 10 kHz. Capacitors from 400 pF to 1 μF are measured in series at 1 kHz and for capacitors greater than 1 μF either series 0.1 kHz or 0.12 kHz can be utilized. For resistance range, resistors less than 1kΩ, can be measured in series 1 kHz. Resistance values from 1 kΩ to 10 MΩ can be measured in parallel at 0.25 kHz. For resistors greater than 10 MΩ parallel mode at 0.03 kHz is suitable. Display range of the unit for the capacitance is from 0.00001 pF to 99999 μF and for the resistance is from 0.00001 Ω to 99999 kΩ. The accuracy for C and R measurements is about 0.05% (basic) + another error term that is defined from a given formula given in the device technical manual (Gwinstek at web site: [www.gwinstek.com.tw]).

The distilled water used in this experiment was produced by an apparatus operating based on the boiling technique, but not a very reliable sample that can be used as a good standard solution. For mineral water a similar brand produced by the same factory is used in all the experiments. The tap water is the regular municipal drinkable city water that is bottled for the all experiments and for boiling water. For the water salt preparation regular grade salt (NaCl) was used for the preparation of a sample with the concentration of about 846 mg/L - 1572 mg/L. For the salt water original solutions with higher concentration was prepared first and then diluted according to the experiment requirement. For water samples care is taken to use similar samples for all the experiments. The salt solutions are prepared carefully to ensure that the concentration of the solution remains constant throughout a series of measurements.

4. Experimental and Theoretical Results:

Using the described experimental setup measurements are performed in turn for the air, distilled, mineral, boiled, tap water, and salt water samples. As mentioned (C,R) pair could be measured simultaneously and temperature is also recorded by another temperature sensor for each measurement. In the first series of experiments similar test samples are used for capacitance/resistance measurements in a single measurement where the resistance and capacitance pair can be monitored simultaneously with the LCR module. Each measurement is repeated at least five times and the average value is plotted. Fig. 3 shows the measured capacitance variation of different samples including air, distilled water (DW) mineral water (MW), tap water (TW), boiled water (BW), and two dilute solutions of salt waters with different salt concentrations(SW1,SW2) for the short probe. Since the capacitance value for the air is much lower than the liquid sample for presentation of all samples in the same figure the measured value for the air capacitance is multiplied by a large number of 10000 as shown in the inset of the Fig.3. As can be seen in Fig.3, the capacitance values plotted here are measured by the LCR module at a fixed temperature of about 15 ˚C and shows increase for the related samples. The capacitance value for the air gap for the short sensor is about 15.3 pF and for the liquids is in the μF range. The measured capacitance when probe is filled with indicated liquid samples are

averaged and for distilled water (DW) is 2.91 µF, for mineral water (MW) is 12.03µF, for tap water (TW) is 12.07 µF, for boiled water (BW) is 12.54 µF, and for dilute solutions of salt water SW1 is 14.73 µF and finally for the SW2 salt water solution is 15.17 µF.

Using similar samples the capacitance measurement is performed with the long probe and the obtained results are shown in Fig.4. As displayed in Fig.4, the measured capacitance values of different samples including air, distilled water (DW) mineral water (MW), tap water (TW), boiled water (BW), and two dilute solutions of salt waters with different salt concentrations(SW1,SW2) for the long cylinder probe are indicated. The capacitance values plotted here are measured by the same LCR module at a fixed temperature of about 15 ˚C for a better comparison. Here like Fig.3, the measured capacitance shows increase for the related samples.

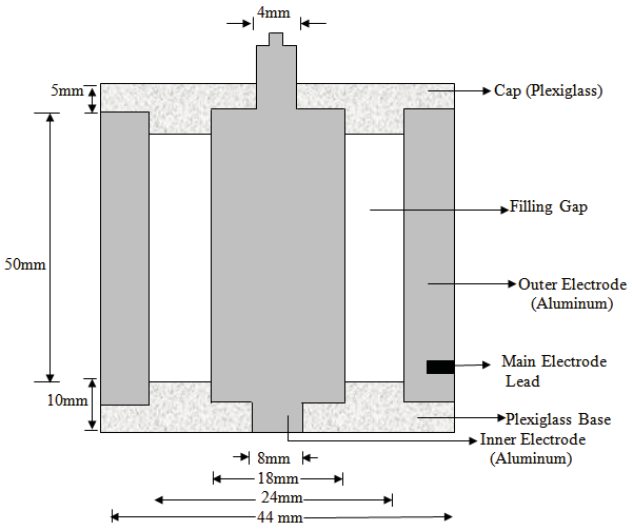

Fig. 1: Design of the cylindrical capacitive cell probe.

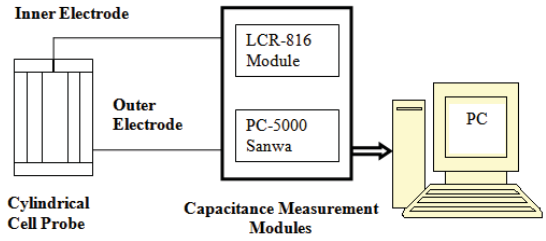

Fig. 2: Block diagram of the experiment for capacitance measurements.

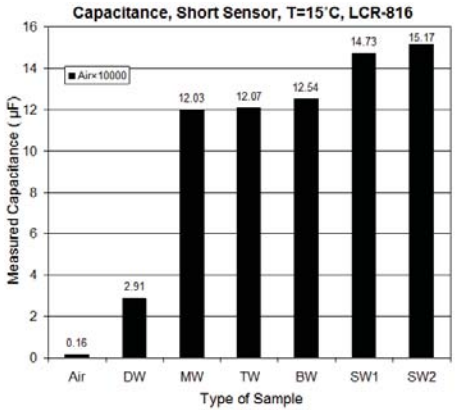

Fig. 3: Capacitance measurements for the air and different water liquids for the short probe.

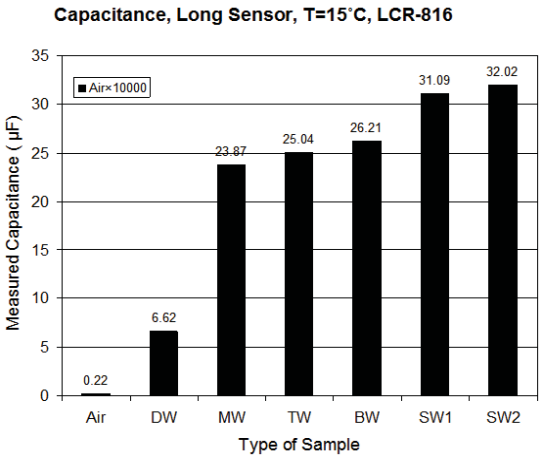

Fig. 4: Capacitance measurements for the air and different water liquids for the long probe.

The capacitance value for the air gap for the long sensor is about 24.7 pF (15.3 pF for the short probe) and for the liquids is again in the µF range. The measured capacitance for the distilled water (DW) is 6.62 µF (2.91 µF for the short probe), for mineral water (MW) is 23.87 µF (12.03µF for the short probe), for tap water (TW) is 25.04 µF (12.07 µF for the short probe), for boiled water (BW) is 26.4 µF (12.54 for the short probe) µF, and for dilute solutions of salt water SW1 is 31.09 (14.73 µF for the short probe) and finally for the SW2 salt water solution is 32.02 µF (15.17 µF for the short probe). In comparing Fig 3 and Fig.4 it is noted that the measured capacitance for all the reported samples for the long sensor is higher, which shows that this quantity increases with the cell length.

Resistance measurements are recorded with the LCR module for both probes and for the short cylinder probe results are shown in Fig.5. As displayed in Fig.5, the measured resistance variation of different samples including air, distilled water (DW) mineral water (MW), tap water (TW), boiled water (BW), and two dilute solutions of salt waters with different salt concentrations (SW1,SW2) are plotted. As can be seen in Fig.5, the resistance values plotted here are measured at a fixed temperature of 15 ˚C for a better comparison.

Since the resistance values for the air and distilled water are much higher than the other samples, hence, for presentation of all samples results in the same figure the measured value for the air resistance is divided by a factor of 100 and for the DW is divided by 10 as shown in the inset of Fig.5. Here unlike Fig.3 and Fig.4, the measured resistance values show decrease for the indicated samples, respectively. The resistance value for the air gap for the short sensor is about 87200 Ω. The measured resistance when probe is filled with indicated liquid samples are averaged and for distilled water (DW) is 2386.2 Ω, for mineral water (MW) is 42.85 Ω, for tap water (TW) is 30.17 Ω, for boiled water (BW) is 27.98 Ω, and for dilute solutions of salt water SW1 is 7.32 Ω, and finally for the SW2 salt water solution is 4.64 Ω.

By using similar samples the resistance measurements are performed with the LCR module and for long probe results are shown in Fig.6. The resistance variation of different samples including air, distilled water (DW) mineral water (MW), tap water (TW), boiled water (BW), and two dilute solutions of salt waters with different salt concentrations(SW1,SW2) are plotted. As can be seen in Fig.6, the resistance values plotted here are measured at a fixed temperature of about 15 ˚C for a better comparison. For presentation of all the samples results in the same figure the measured value for the air resistance is divided by 100 and for DW is divided by 10. Here the measured resistance values show decrease for the indicated samples.

The resistance value for the air gap for the long sensor is about 29824 Ω (87200 Ω for the short probe). The measured resistance when probe is filled with indicated liquid samples are averaged and for distilled water (DW) is 1217.4 Ω (2386.2 Ω for the short probe), for mineral water (MW) is 21.05 Ω (42.85 Ω for the short probe), for tap water (TW) is 14.95 Ω (30.17 Ω for the short probe), for boiled water (BW) is 13.57 Ω (27.98 for the short probe), and for dilute solutions of salt water SW1 is 3.5 Ω (7.32 Ω for the short probe) and finally for the SW2 salt water solution is 2.2 Ω (4.64 Ω for the short probe). In comparing Fig. 5 and Fig.6 it is noted that the resistance values for all samples for the long sensor is lower, which shows that the measured resistance decreases with the cylindrical cell length.

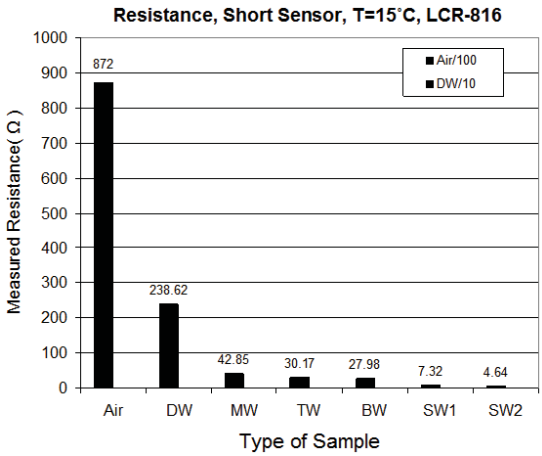

Fig. 5: Resistance measurements for the air and different water liquids for the short probe.

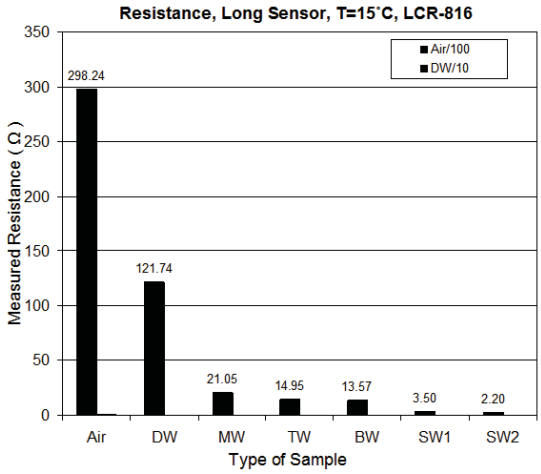

Fig. 6: Resistance measurements for the air and different water liquids for the long probe.

In the next study the goal is to find how the probe length affects the capacitance and resistance measurements for the described probes in liquid filling process. Fig.7 shows the measured capacitance values for the two cylindrical sensors filled with distilled water. Here measurements are performed with the LCR module for both probes and similar water samples are used as the filling medium of the gap. It must be mentioned that the cylindrical gap volume for the long probe is 20 cc and for the short probe is about 10 cc. In this experiment certain amount of water is poured in the cylinder gap and the related capacitance/resistance values are measured simultaneously. The capacitance values plotted here are measured at a fixed temperature of 15 ˚C. The behavior of the response curves are very similar for different water volumes for the two probes and show a nearly capacitance increase with the increase of water sample volume. For the short cylindrical probe at 10 cc volume the whole gap is filled with the water sample (full-filled) while for the long probe there is an empty air gap of 10 cc in volume as well as the water filled gap of 10 cc (half-filled).

As can be seen in Fig. 7, for distilled water (DW) capacitance for 1 cc water filling is about 0.6 μF for the long probe and 0.5 μF for the short probe. For a water volume of about 4 cc the capacitance increases to about 1.5 μF for the both probes and finally 3.5 μF for the short probe and to about 4 μF for the long probe at 10 cc water filling. As shown in Fig.7, for different water fillings there is a good agreement between the results obtained for the two different probes for the case of filling a small amount of the water to the air gap. The reason is that major part of the gap is filled with the air and as can be seen up to a volume of 5 cc, a linear increase in the measured capacitance is observed. However, for further water filling the behavior of the

long probe is different from the short probe. The result of this study shows that the probe length does have an effect on the capacitance measurements for partially-filled or full-filled probes.

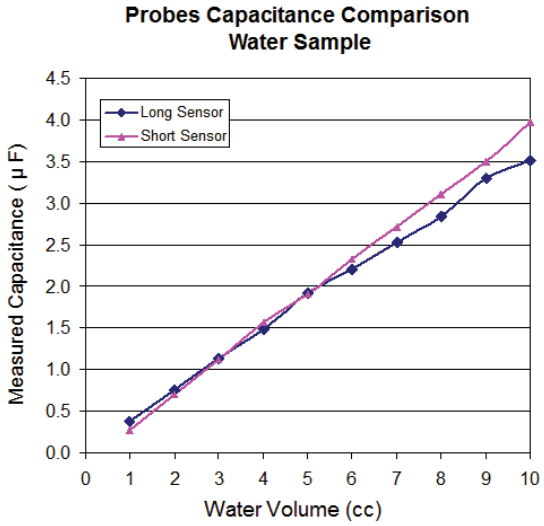

Fig. 7: Capacitance variation for different volumes distilled water liquid filling.

In Fig. 8 the measured resistance values for the two cylindrical sensors in filling with distilled water are presented. As can be seen in Fig.8, the resistance values plotted here are measured at a fixed temperature of about 15 ˚C. The measured resistance when probe is filled with indicated liquid sample show a decrease by increasing the gap liquid volume and the reason is that the dielectric constant of the water is higher and as a result the resistance value of the water sample is higher than that of the air gap. As can be seen in Fig. 8, for distilled water (DW) resistance for 1 cc water filling is about 23 kΩ for the long probe and 28 kΩ for the short probe. For a water volume of about 5cc the resistance decreases to about 5 kΩ for the both probes and finally decreases to about 3 kΩ for the 10 cc water filling. For the short cylindrical probe at 10 cc volume the whole gap is filled with the water sample while for the long probe there is an half-empty. As shown in Fig.8, for different water fillings there is a good agreement between the results obtained for the two different probes for the full-filling case while the responses of the two probes are different for the partial-filling conditions. The result for resistance changes shows that the probe length affects the resistance value for the partial filling of the probe, but similar behavior is observed for the full-filling of distilled water. The overall results of this liquid filling investigation displayed in Fig.7 and Fig.8 show that the probe length have a role on the capacitance and resistance measurements of the probes for partial- and full- fillings of water liquid.

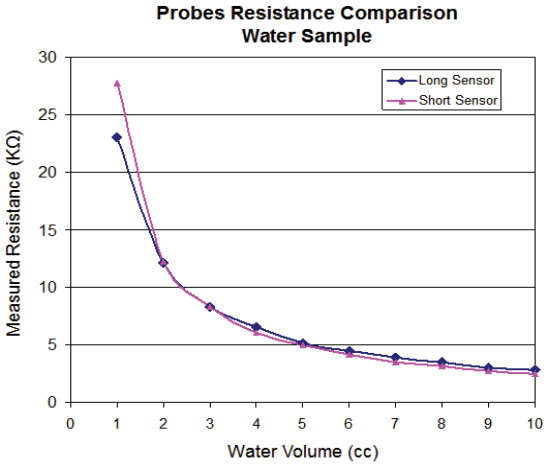

Fig. 8: Resistance variation for different volumes distilled water liquid filling.

In order to compare experimental results with the theoretical calculations in the next study we describe the computed results based on the Gauss and Coulomb theories. The computed results according to Gauss law given by Eq. (1) and for Coulomb law according to Eq. (7) are obtained. In Fig.9, capacitance per unit length is computed from described theories and compared. As expected from Eq.(1) and as shown in Fig.9, capacitance per unit length from Gauss theory is a constant value of about 193 F while for the Coulomb theory starts from 720 pF/m and a length of about 200 pF/m. as can be seen in Fig.9, as expected there is a good agreement between the Coulomb and Gauss theories at longer lengths while a big deviation is noticed at short capacitor lengths. For example, for the length range of 0.005 m (5mm) to 0.05 m (50 mm) the values given by Coulomb law are more accurate. However, as mentioned for longer length values the computed results reach a similar value.

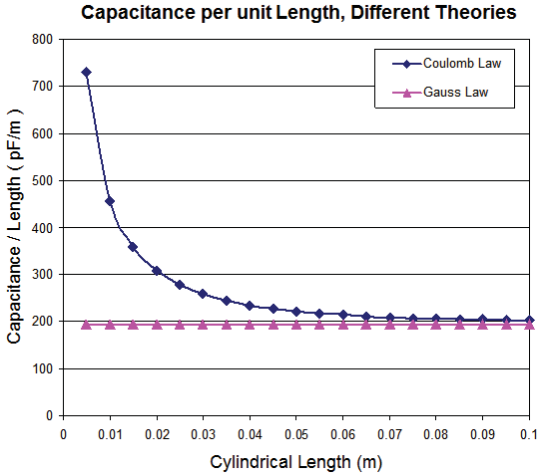

Fig. 9: Computed air capacitance per unit length from two theories.

In Fig.10, computed capacitance values as a function of the cylinder length are presented for the length range of 0.5 to 10 cm, which corresponds to the tested experimental cylindrical cells. As expected from Eq.(1) and Eq.(7) the capacitance value increases almost linearly with the cylinder length as shown in Fig.10. However the slope of the capacitance increase as indicated in Fig.10 is higher for the Coulomb law in comparison with the Gauss theory. As shown in Fig.10, a big deviation in the computed results is noted at small length values while the capacitance variation lines approaching each other at higher length values. As a result disagreement in results is more notable at shorter cell lengths while at longer length values (>10 cm) the Gauss law results approaching the Coulomb's law, which provides more precise capacitance values for all length values. The concluding remark of this theoretical study is that according to the given results for the air gap capacitance; selection of a precise formulation is unavoidable for the shorter lengths and as described Coulomb law provides a more accurate computed value for the capacitance analysis.

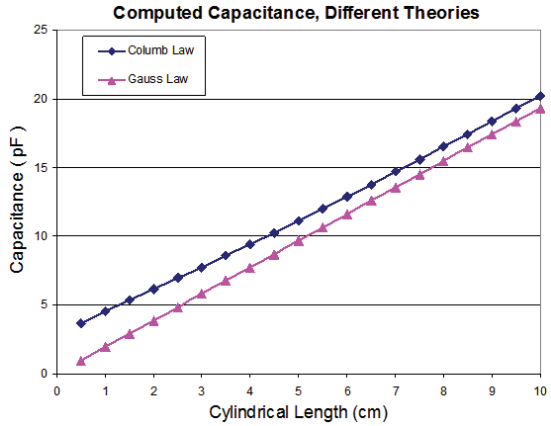

Fig. 10: Computed air capacitance values from two theories.

Table1 shows the capacitance per unit length computed form Gauss and Coulomb theories for the air gap using the short and long probes. As can be seen in Table1, as expected, capacitance per unit length from the Coulomb theory is different from the Gauss law. For air gap such a quantity from gauss law is a constant value of about 193.29 pF/m while for the Coulomb theory for the long probe (L=10 cm) is 202.08 pF/m and from experiment is about 247 pF/m. For the short probe also the results from the Coulomb theory is different from the Gauss law. For air gap such a quantity from Gauss law is a constant value of about 193.29 pF/m while for the Coulomb theory for the short probe is 222.08 pF/m and from experiment for this probe is about 306 pF/m.

Table 1: Comparison of air capacitance measurement and calculated ones for two probes.

Capacitance Probe Type	Gauss Law C_g (pF),	Coulomb Law C_c(pF)	Experiment C_e(pF) T=15°C	Rel. Error (%) $(C_e-C_c)/Ce$
Long Cylinder (L= 10 cm)	19.329	20.208	22.6	10.58
Short Cylinder (L= 5 cm)	9.664	11.123	15.3	27.3

Capacitance results for the short and long probes for the air gap are compared in Table 2 with the experimental results. Table2 shows the capacitance values computed form Gauss and Coulomb theories for the air gap. As can be seen in Table2, as expected, capacitance values for both probes from the Coulomb theory is different from the Gauss law. For air gap for the long probe Gauss law gives is a capacitance value of about 19.329 F while from the Coulomb theory is 20.208 pF and from experiment is about 24.7 pF. For the short probe also the results from the Coulomb theory is different from the Gauss law. For air gap such a quantity from Gauss law is about 9.664 pF while from Coulomb theory is 11.123 pF and from experiment for this probe is about 15.3 pF.

Table 2: Comparison of measured air capacitance per unit length and calculated ones for two probes.

Capacitance/Length Probe Type	Gauss Law C_g (pF),	Coulomb Law C_c(pF)	Experiment C_e(pF) T=15°C	Rel.Error (%) $(C_e-C_c)/Ce$
Long Cylinder (L= 10 cm)	193.29	202.08	226	10.58
Short Cylinder (L= 5 cm)	193.29	222.8	306	27.18

In comparing the given results in Table 1 and Table 2 two main points can be concluded. First, for both probes the results from Coulomb theory are closer to the obtained experimental results. Second, deviation of the experimental results from both theories, in particular Gauss law is more severe for the short probe design. As expected Gauss law is only valid for the case that the length of the cylinder is much higher than the radii of the inner and outer electrodes. To show such a deviation the relative error percentages are also listed in Table 1 and 2 for both cylindrical probes. As can be seen in Tables, the experimental results are closer to the theoretical values obtained by Coulomb law. Comparing the experimental capacitance results with Coulomb theory shows a relative error percentage of 18.18% for the long probe and a relative error percentage of 27.32% for the short probe.

Since the DMM (SANWA) capacitance measuring module can be interfaced to a PC computer so it is possible to investigate the time variation of the reactance capacitance and resistance by using such a measuring module. For example the development of the conduction lines from liquid to metal electrodes can be investigated by this module and can be monitored on PC display unit. On the other hand dynamic behavior of the touching liquid with the metallic electrodes and development of the conduction term in capacitance can be investigated by this real-time measurement scheme. Fig.11 shows the variation of the measured capacitance for the water samples. In the first part of a few milliseconds the conduction is not formed and as a result the reactance capacitance is negligible, but after a time scale of about few seconds the resistance and as a result the reactance term is fully developed and in such condition the dielectric capacitance is negligible as can be seen in Fig.11. For a longer time the reactance capacitance is reaching the steady-state condition and the measured value is almost constant with time. As expected any increase in conductance term will cause a reduction in the resistance of the filling water sample.

Fig.12 shows the time variation of the measured resistances for different water samples using DMM module. In the first part of a few milliseconds the conduction is not formed and as a result the resistance is high, but after a time scale of about few seconds the conductance term is fully developed and in such condition the dielectric capacitance is negligible as can be seen in Fig.12 and the resistance value remains almost as a constant value. For a longer time the resistance part is reaching the steady-state condition and the measured values are almost constant with time. As expected any increase in conductance term will cause a reduction in the resistance of the water sample as can be noted in Fig.12.

As shown in Fig.12, the resistance variation for the distilled water (DW) is more notable in comparison with the MW, BW, and TW samples. For instance for DW the resistance starts from 1818.6 kΩ and drops to a value of about 548.0 kΩ in a time scale of 50 s. For this period of time MW shows a resistance change from 293.95 kΩ to 191.76 kΩ, BW from 385.05 kΩ to 248.81 kΩ and finally TW shows a variation from 36.1 kΩ to 25.42 kΩ for the same time scale. Another advantage of such an investigation is the fact that can lead to useful information about the electrical conduction interaction of different sample liquids with various metallic electrodes at the early stage of liquid wetting of the electrodes.

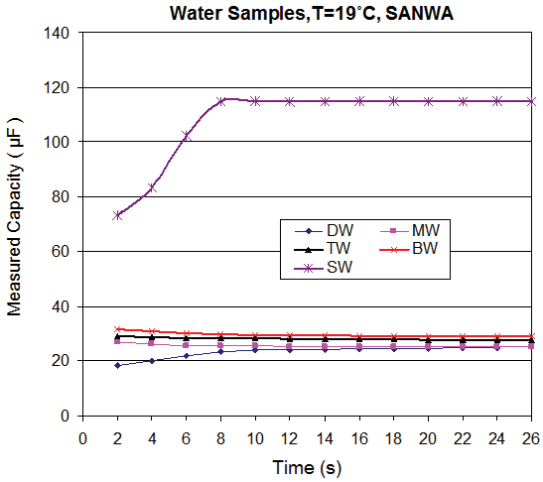

Fig. 11: Time variation of the measured capacitance for the water samples.

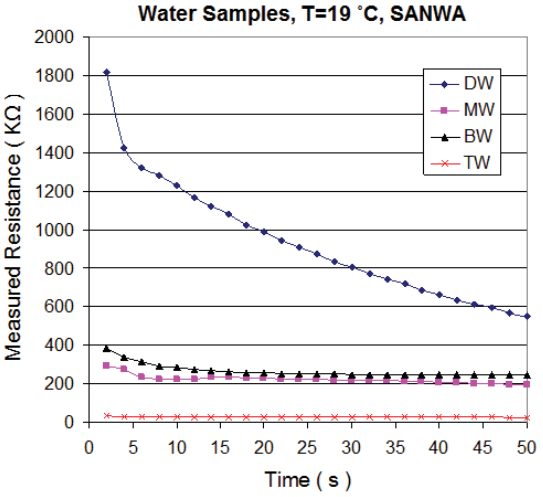

Fig. 12: Time variation of the measured resistances for different water samples using DMM module.

In comparison with other results it must be pointed out that some physical parameters of the water liquids is reported in literature. For example, capacitance sensors for measurement of phase volume fraction in two-phase pipelines have been reported (Strizzolo and Cinverti, 1993). Persson, and Haridy in year 2003 reported a paper titled as estimating water content from electrical conductivity measurements with short time-domain reflectometry probes (Persson and Haridy, 2003). Some general information concerning different aspect of the water liquid is given in Handbook of Chemistry and Physics (Weast, 1981).

One might ask why there are differences in capacitance and resistance values for the same water samples when using different measuring modules. As a first point, it must be mentioned that in both cases the measured values are just the measured capacitance and resistance figures, which are in general different from the actual capacitance and resistance of the filling liquid. The measured values for air gap can be correlated to the

measured values, however as described in section 3 the measured values depends on the measurement techniques. Here the LCR module uses the resonant method while the SANWA operates based on the charge/discharge method. Second point is that as mentioned the measured values depend on the frequency of the measurement that are different for the two modules. LCR measurements are for the range of 1 kHz while for the SANWA are at lower frequency range of Hz. The reactance capacitance and as a result the resistance term is inversely proportional to the frequency and as can be seen from results the resistance values given by LCR module is much lower than values measured by the SANWA module for the similar sample types. However, for comparison of the results for two different lengths as long as measurements quoted for both cells are done by the same module are quiet reasonable.

To sum up our result discussions the main parameters of the reported investigation are compared in different tables. In Table 3 conductivity and resistance values for the short sensor are listed. Conductivity and Total Dissolved Solid (TDS) values listed in Table 3 for the given samples are measured by EC at the room temperature. As can be seen increasing the TDS value will increase the conductivity and inversely the resistance value is decreased. The measured resistance value for each sample measured with the LCR module using the short probe filled with sample liquid is shown respectively. For a better comparison the mineral water is considered as the reference sample, because it is more reproducible in our experiments and the conductance ratio and resistance ratio normalized to this reference are compared for different samples. As can be seen in Table 3, in the conductance ratios obtained with the EC and resistance ratios determined by our measurements by LCR a good agreement is observed. For instance for distilled water, tap water, boiled water the ratios are exactly the same, while for the salt water a minor difference is observed.

Table 3: Conductivity and resistance values for the short sensor.

Water Sample	Conductivity (μS/cm),EC,T=20.6°C	TDS (mg/L),EC T=20.6°C	Resistance (Ω), LCR T=15°C	G/G_m	R_m/R
Distilled	3.41	1.7	1287	0.015	0.016
Mineral	223	111.4	20.72	1	1
Tap	318	158.8	14.8	1.4	1.4
Boiled	341	170.6	13.64	1.5	1.5
Salt Water1	1693	846	3.49	7.5	5.9
Salt Water2	3140	1572	2.21	14	9.3

G,R(sample; G_m,R_m (Mineral water)

In order to compare the conductance results in Table 4 a comparison of conductivity and relative error percentage for the short sensor is given. As can be seen there is a good agreement between the measured results by the EC and the cylindrical cell probe, in particular for the distilled, mineral, tap and boiled water samples. As indicated in Table 4 the relative errors for the given samples are lower than 2% for the mentioned plane waters. However, for the salt water samples the deviation in results of two measurements are more notable, which is due to enhanced conductance effects for such salt water solutions.

Similar comparison in measured results is considered for the long probe. The conductivity, and TDS of different samples listed in Table 5 are measured using the EC system at the room temperature. The results of such measurements along with the results obtained from our cylindrical cell probe are compared in Table 5. As can be seen increasing the TDS value will increase the conductivity and inversely the resistance value is decreased for the given samples. The resistance value for each sample measured with the LCR module using the long probe is shown respectively. For a better comparison the mineral water is considered as the reference sample as before and the conductance ratios and resistance ratios are compared for different samples. As can be seen in the conductance ratios obtained with the EC and resistance ratios determined by measurements by LCR a good agreement is observed. For example, for distilled water, tap water, and the boiled water the ratios are exactly the same, while for the salt water samples minor differences are observed.

Table 4: Computation of conductivity and relative error percentage for short sensor.

Water Sample	G(μS/cm)	G´(μS/cm)	Difference (G- G´)*	Error (%) (G- G´)/G
Distilled	3.41	3.35	0.09	-1.7
Mineral	223	223	0	0
Tap	318	312.2	5.8	-1.8
Boiled	341	334	7	-2
Salt Water1	1693	1316	377	-22
Salt Water2	3140	2029	1111	-35

*__G__: Conductivity measured with EC Meter, __G´__: Conductivity measured with Cell Probe

Table 5: Conductivity and TDS values for given samples filling the long cell probe.

Water Sample	Conductivity (μS/cm),EC, T=20.6°C	TDS (mg/L),EC,T=20.6°C	Resistance (Ω), LCR T=15°C	G/GM	RM/R
Distilled	3.41	1.7	2743	0.015	0.015
Mineral	223	111.4	42.14	1	1
Tap	318	158.8	30.11	1.4	1.4
Boiled	341	170.6	28.22	1.5	1.5
Salt Water1	1693	846	7.17	7.5	5.9
Salt Water2	3140	1572	4.65	14	9.1

G,R(sample); G_M,R_M (Mineral water)

Table 6: Conductivity and relative error percentage for the long sensor.

Water Sample	G(μS/cm)	G′(μS/cm)	Difference (G- G′)*	Error (%) (G- G′)/G
Distilled	3.41	3.5	0.09	2
Mineral	223	223	0	0
Tap	318	312.2	5.8	-1.8
Boiled	341	334	7	-2
Salt Water1	1693	1316	377	-22
Salt Water2	3140	2074	1066	-33

*G: Conductivity measured with EC Meter, **G′**: Conductivity measured with Cell Probe

Similar to the case of the short probe in order to compare the conductance results in Table 6 a computation of conductivity and relative error percentage for the long sensor are listed. As can be seen, there is a good agreement between the measured results by the EC and the cell probe, in particular for the distilled, mineral, tap and boiled water samples. As shown in Table 6 the relative errors for the given samples are lower than 2% for the mentioned plane waters. However, As described before for the salt water samples the differences in results are more pronounced (higher than 22%), which is due to the enhanced conductance effects for such samples.

5. Conclusions:

The goal here was to implement new capacitance cell probes to see the probe length effects on the results for air gap and liquid-filled gap. It was noted that the invasive type sensor such as the one reported here provides a useful means to study the resistance and reactance capacitance and its role in the capacitance measurements. The length dependence of the capacitance values for the air and liquid filling are investigated and compared in this study. Obtained results verified that the reported sensor could be effectively implemented for the study of low conducting liquids such as regular tap water and water solutions. On the other hand, this method provides a sensitive way to measure the effect of the cell length for air and liquid filling of liquid by considering the conductance and resistance measurements performed by using the reactive capacitance variations. The comparison of the results clearly shows the validity of the Gauss's law in computation of the cell probe capacitance by comparing the results for the short and long probe cells.

As expected, capacitance per unit length from the Coulomb theory is different from the Gauss law. For air gap such a quantity from gauss law is a constant value of about 193 F/m while for the Coulomb theory starts from 720 pF/m and decreases to a value of about 200 pF/m for a length of 0.1 m. A measured air capacitance of (247 pF) and calculated ones (Gauss, 193.29 pF, Coulomb, 247 pF) for the long probe is obtained. For the short probe respected capacitances are (193.29 pF) from measurements, from Gauss law (222.8 pF), and (306 pF) from the Coulomb theory. As a result the theoretical values obtained by Coulomb law are closer to the experimental results for the two probes and comparing the experimental capacitance results with Coulomb theory shows a relative error percentage of 18.18% for the long probe and an error of 27.32% for the short probe. For different water liquids and salt waters, dilute salt water shows a factor of 78.08% increase in measured reactance capacitance in respect to distilled water and 20.69% increase in comparison with the mineral water at temperature of 15.0 ˚C. For the same samples for the long probe the dilute salt water shows a factor of 79.32% increase in measured reactance capacitance in respect to distilled water and 25.45 % increase in comparison with the mineral water at similar temperature. Hence the reported cell probe provides a relatively accurate method to determine the length effects for the air, liquid samples, and also liquids with a trace impurity.

For liquid samples conductivity and TDS values listed in Table 3 and Table 5 for the given samples are measured by EC at the room temperature. The measured resistance value for each sample measured with the LCR module using the short probe filled with sample liquid is shown respectively. The mineral water is considered as the reference sample, because it is more reproducible in our experiments and the conductance ratio and resistance ratio normalized to this reference are compared for different samples. As can be seen in

Table 3, in the conductance ratios obtained with the EC and resistance ratios determined by our measurements by LCR a good agreement is observed. As described for distilled water, tap water, boiled water the ratios are exactly the same, while for the salt water a minor difference is observed.

In order to compare the conductance results in Table 4 a comparison of conductivity and relative error percentage for the short sensor is given. As can be seen there is a good agreement between the measured results by the EC and the cylindrical cell probe, in particular for the distilled, mineral, tap and boiled water samples. As indicated in Table 4, and Table 6 the relative errors for the given samples are lower than 2% for the mentioned plane waters. However, for the salt water samples the deviations in results of two measurements are more notable, which is due to enhanced conductance effects for such salt water solutions. In comparing the results for the short (Tables 3,4) and long probes (Tables 5,6) it is noted the length effect caused more deviations in the results for the salt water solutions, which clearly indicates the role of the probe length in such measurements.

ACKNOWLEDGEMENTS

The authors like to acknowledge the support given by the office of vice president for research and technology of the Sharif University of Technology.

REFERENCES

Ahn, H-J., I-H. Kim and D-C. Han, 2005. Nonlinear analysis of cylindrical capacitive sensor. Meas. Sci. Technol., 16: 699-706.

Behzadi, G. and H. Golnabi, 2009. Monitoring temperature variation of reactance capacitance of water using a cylindrical cell probe. J. of Applied Sciences, 9: 752-8.

Fasching, G.E., W.J. Loudin and N.S. Smith, 1994. Capacitance system for three-dimensional imaging of fluidized-bed density. IEEE Trans. On Instrumentation and Measurement, 43: 56-62.

Golnabi, H. and P. Azimi, 2008. Design and performance of a cylindrical capacitive sensor to monitor the electrical properties. J. of Applied Sciences, 8: 1699-1705.

Golnabi, H. and P. Azimi, 2008. Simultaneous measurements of the resistance and capacitance using a cylindrical sensor system. Modern Physics Letter, B 22: 595-610.

Gwinstek at web site: [www.gwinstek.com.tw].

Guo, S., J. Guo and W.H. Ko, 2000. A monolithically integrated surface micromachined touch mode capacitive pressure sensor. Sens. Actuators A 80: 224-32.

Huang, S.M., A.L. Stott, R.G. Green and M.S. Beck, 1988. Electronic transducers for industrial measurement of low value capacitances. J. Phys. E: Sci. Instrum., 21: 242-50.

Huang, S.M., R.G. Green, A.B. Plaskowski and M.S. Beck, 1988. Conductivity effects on capacitance measurements of two-component fluids using the charge transfer method. J. Phys. E: Sci. Instrum., 21: 539-48.

Kasten, K., J. Amelung and W. Mokawa, 2000. CMOS-compatible capacitive high temperature pressure sensors. Sens. Actuators A., 85: 147-52.

Light, T.S., S. Licht, A.C. Bevilacqua and K.R. Morash, 2005. The fundamental conductivity and resistivity of water. Electrochemical and Solid-state letter, 8: E16-E19.

McIntosh, RB., P. E. Mauger and S.R. Patterson., 2006. Capacitive transducers with curved electrodes. IEEE, sensors., 6: 125-38.

Moe, S.T., K. Schjolberg-Henriksen, D.T. Wang, E. Lund, J. Nysaether, L. Fruberg, M. Visser, T. Fallet, and R.W. Bernstein, 2000. Capacitive differential pressure sensor for harsh environments, Sens. Actuators A 83: 30-3.

Rodjegard, H and A. Loof, 2005. A differential charge-transfer readout circuit for multiple output capacitive sensors. Sens. Actuators A., 119: 309-15.

Sanwa at web site: [http://www.sanwa-meter.co.jp/overseas/].

Persson, M. and S. Haridy, 2003. Estimating water content from electrical conductivity measurements with short time-domain reflectometry probes, Soil. Sci. Soc., 67: 478-82.

Strizzolo, C.N. and J. Cinverti, 1993. Capacitance sensors for measurement of phase volume fraction in two-phase pipelines. IEEE Trans. On Instrumentation and Measurement., 42: 726-9.

Tsamis, E.D. and J.N. Avaritsiotis, 2005. Design of a planar capacitive type senor for water content monitoring in a production line. Sens. Actuators A 118: 202-11.

Weast, R.C., 1981. Handbook of Chemistry and Physics, 60 th. Ed., CRC Press, E-61.